

Cite as: T. Lecocq *et al.*, *Science*
10.1126/science.abd2438 (2020).

Global quieting of high-frequency seismic noise due to COVID-19 pandemic lockdown measures

Thomas Lecocq^{1*}, Stephen P. Hicks², Koen Van Noten¹, Kasper van Wijk³, Paula Koelemeijer⁴, Raphael S. M. De Plaen⁵, Frédéric Massin⁶, Gregor Hillers⁷, Robert E. Anthony⁸, Maria-Theresia Apoloner⁹, Mario Arroyo-Solórzano¹⁰, Jelle D. Assink¹¹, Pinar Büyükkakpınar^{12,13}, Andrea Cannata^{14,15}, Flavio Cannavo¹⁵, Sebastian Carrasco¹⁶, Corentin Caudron¹⁷, Esteban J. Chaves¹⁸, David G. Cornwell¹⁹, David Craig²⁰, Olivier F. C. den Ouden^{11,21}, Jordi Diaz²², Stefanie Donner²³, Christos P. Evangelidis²⁴, Láslo Evers^{11,21}, Benoît Fauville²⁵, Gonzalo A. Fernandez²⁶, Dimitrios Giannopoulos^{27,28}, Steven J. Gibbons²⁹, Társilo Girona³⁰, Bogdan Grecu³¹, Marc Grunberg³², György Hetényi³³, Anna Horleston³⁴, Adolfo Inza³⁵, Jessica C. E. Irving^{34,36}, Mohammadreza Jamalrehyani^{37,13}, Alan Kafka³⁸, Mathijs R. Koymans^{11,21}, Celeste R. Labeledz³⁹, Eric Larose¹⁷, Nathaniel J. Lindsey⁴⁰, Mika McKinnon^{41,42}, Tobias Megies⁴³, Meghan S. Miller⁴⁴, William Minarik^{45,46}, Louis Moresi⁴⁴, Víctor H. Márquez-Ramírez⁵, Martin Möllhoff²⁰, Ian M. Nesbitt^{47,48}, Shankho Niyogi⁴⁹, Javier Ojeda⁵⁰, Adrien Oth⁵¹, Simon Proud⁵², Jay Pulli^{53,38}, Lise Retailleau^{54,55}, Annukka E. Rintamäki⁷, Claudio Satriano⁵⁴, Martha K. Savage⁵⁶, Shahar Shani-Kadmiel²¹, Reinoud Sleeman¹¹, Efthimios Sokos⁵⁷, Klaus Stammer²³, Alexander E. Stott⁵⁸, Shiba Subedi³³, Mathilde B. Sørensen⁵⁹, Taka'aki Taira⁶⁰, Mar Tapia⁶¹, Fatih Turhan¹², Ben van der Pluijm⁶², Mark Vanstone⁶³, Jerome Vergne⁶⁴, Tommi A. T. Vuorinen⁷, Tristram Warren⁶⁵, Joachim Wassermann⁴³, Han Xiao⁶⁶

¹Seismology-Gravimetry, Royal Observatory of Belgium, Avenue circulaire 3, 1180 Brussels, Belgium. ²Department of Earth Science and Engineering, Imperial College London, London, UK. ³Department of Physics, University of Auckland, New Zealand. ⁴Department of Earth Sciences, Royal Holloway University of London, Egham, UK. ⁵Centro de Geociencias, Universidad Nacional Autónoma de México, Campus Juriquilla, Querétaro, Mexico. ⁶Swiss Seismological Service, ETH Zurich, Sonneggstrasse 5, CH-8092, Zurich, Switzerland. ⁷Institute of Seismology, University of Helsinki, Helsinki, Finland. ⁸U.S. Geological Survey - Albuquerque Seismological Laboratory, New Mexico, USA. ⁹Zentralanstalt für Meteorologie und Geodynamik (ZAMG), Vienna, Austria. ¹⁰Escuela Centroamericana de Geología, Universidad de Costa Rica, San José, Costa Rica. ¹¹R&D Seismology and Acoustics, Royal Netherlands Meteorological Institute (KNMI), Utrechtseweg 297, 3731 GA De Bilt, Netherlands. ¹²Kandilli Observatory and Earthquake Research Institute, Boğaziçi University, Istanbul, Turkey. ¹³GFZ German Research Centre for Geosciences, Potsdam, Germany. ¹⁴Dipartimento di Scienze Biologiche, Geologiche e Ambientali, Università degli Studi di Catania, Catania, Italy. ¹⁵Istituto Nazionale di Geofisica e Vulcanologia, Osservatorio Etno, Catania, Italy. ¹⁶Bensberg Observatory, University of Cologne, Cologne, Germany. ¹⁷Univ. Grenoble Alpes, Univ. Savoie Mont Blanc, CNRS, IRD, IFSTTAR, ISTerre, 38000 Grenoble, France. ¹⁸Volcanological and Seismological Observatory of Costa Rica at Universidad Nacional (OVSICORI-UNA), Costa Rica. ¹⁹Department of Geology & Geophysics, School of Geosciences, University of Aberdeen, King's College, Aberdeen, AB24 3UE, UK. ²⁰Dublin Institute for Advanced Studies, Geophysics Section, 5 Merrion Square, D02 Y006 Dublin, Ireland. ²¹Dept. of Geoscience and Engineering, Delft University of Technology, Stevinweg 1, 2628 CN Delft, Netherlands. ²²Geosciences Barcelona, CSIC, Barcelona, Spain. ²³Federal Institute for Geosciences and Natural Resources (BGR), Hannover, Germany. ²⁴Institute of Geodynamics, National Observatory of Athens, Greece. ²⁵Noise Department, Brussels Environment, Brussels-Capital Region, Belgium. ²⁶Observatorio San Calixto, Bolivia. ²⁷Seismotech S.A., Athens, Greece. ²⁸Hellenic Mediterranean University, Dept. of Environmental & Natural Resources Engineering, Laboratory of Geophysics & Seismology, Chania, Greece. ²⁹Norges Geotekniske Institutt, Sognsveien 72, 0855 Oslo, Norway. ³⁰Geophysical Institute, University of Alaska Fairbanks, Alaska 99775, USA. ³¹National Institute for Earth Physics, Calugareni 12, Magurele, Romania. ³²Réseau National de Surveillance Sismique (RENASS); Université de Strasbourg, CNRS, EOST UMS830, 5 rue René Descartes, F-67084 Strasbourg Cedex, France. ³³Institute of Earth Sciences, Faculty of Geosciences and Environment, University of Lausanne, Lausanne, Switzerland. ³⁴School of Earth Sciences, University of Bristol, Queen's Road, Bristol, BS8 1RJ, UK. ³⁵Instituto Geofísico del Perú, Lima, Peru. ³⁶Department of Geosciences, Princeton University, NJ, USA. ³⁷Institute of Geophysics, University of Tehran, Iran. ³⁸Weston Observatory, Department of Earth and Environmental Sciences, Boston College, Weston, MA, USA. ³⁹Seismological Laboratory, California Institute of Technology, Pasadena, CA, USA. ⁴⁰Geophysics Department, Stanford University, Stanford, CA, USA. ⁴¹SETI Institute, Mountain View, CA, USA. ⁴²Faculty of Science, Department of Earth, Ocean and Atmospheric Sciences, University of British Columbia, Canada. ⁴³Ludwig-Maximilians-Universität München, Munich, Germany. ⁴⁴Research School of Earth Sciences, Australian National University, Canberra, ACT Australia. ⁴⁵Department of Earth and Planetary Sciences, McGill University, Montréal, QC, Canada. ⁴⁶GEOTOP Research Centre, Montréal, QC, Canada. ⁴⁷Raspberry Shake, S.A. ⁴⁸Department of Earth and Climate Science, University of Maine, Orono, ME, USA. ⁴⁹University of California, Riverside, USA. ⁵⁰Departamento de Geofísica, Universidad de Chile, Santiago, Chile. ⁵¹European Center for Geodynamics and Seismology; 19, rue Josy Welter; L-7256 Walferdange, Grand Duchy of Luxembourg. ⁵²National Centre for Earth Observation, Department of Physics, University of Oxford, UK. ⁵³Raytheon BBN Technologies, Arlington, VA, USA. ⁵⁴Université de Paris, Institut de physique du globe de Paris, CNRS, F-75005 Paris, France. ⁵⁵Observatoire Volcanologique du Piton de la Fournaise, Institut de physique du globe de Paris, F-97418 La Plaine des Cafres, France. ⁵⁶School of Geography, Environment and Earth Sciences, Victoria University of Wellington, New Zealand. ⁵⁷Department of Geology, University of Patras, Patras, 26504 Rio, Greece. ⁵⁸Department of Electrical and Electronic Engineering, Imperial College London, South Kensington Campus, London, SW7 2AZ, UK. ⁵⁹Department of Earth Science, University of Bergen, Bergen, Norway. ⁶⁰Berkeley Seismological Laboratory, University of California Berkeley, Berkeley, USA. ⁶¹Laboratori d'Estudis Geofísics Eduard Fontserè, Institut d'Estudis Catalans (LEGF-IEC), Barcelona, Spain. ⁶²Department of Earth and Environmental Sciences, University of Michigan-Ann Arbor, MI, USA. ⁶³Geology Department, Truro School, Trennick Lane, Truro, Cornwall, TR1 1TH, UK. ⁶⁴Institut de Physique du Globe de Strasbourg; UMR 7516, Université de Strasbourg/EOST, CNRS; 5 rue René Descartes, F-67084 Strasbourg Cedex, France. ⁶⁵Department of Physics, University of Oxford, UK. ⁶⁶Department of Earth Science and Earth Research Institute, University of California, Santa Barbara, CA, USA.

*Corresponding author. Email: thomas.lecocq@seismology.be

Human activity causes vibrations that propagate into the ground as high-frequency seismic waves. Measures to mitigate the COVID-19 pandemic caused widespread changes in human activity, leading to a months-long reduction in seismic noise of up to 50%. The 2020 seismic noise quiet period is the longest and most prominent global anthropogenic seismic noise reduction on record. While the reduction is strongest at surface seismometers in populated areas, this seismic quiescence extends for many kilometers radially and hundreds of meters in depth. This provides an opportunity to detect subtle signals from subsurface seismic sources that would have been concealed in noisier times and to benchmark sources of anthropogenic noise. A strong correlation between seismic noise and independent measurements of human mobility suggests that seismology provides an absolute, real-time estimate of population dynamics.

Seismometers record signals from more than just earthquakes; interactions between the solid Earth and fluid bodies, such as ocean swell and atmospheric pressure (1, 2), are now commonly used to image and monitor the subsurface (3). Human activity is a third source of seismic signal. Nuclear explosions and fluid injection/extraction result in impulsive signals, but everyday human activity is recorded as a near-continuous signal especially on seismometers in urban environments. These complicated signals are the superposition of a wide variety of activities happening at different times and places at or near the Earth's surface, but are typically stronger during the day than at night, weaker on weekends than weekdays, and stronger near population centers (4–7). Seismometers in urban environments are important to maximize the spatial coverage of seismic networks and to warn of local geologic hazards (8), even though anthropogenic seismic noise degrades their capability to detect transient signals associated with earthquakes and volcanic eruptions. Understanding urban seismic sources is therefore vital. However, research studies have been limited to confined areas or distinct events, such as road traffic (9, 10), public transport (7, 11), and “football quakes” (11, 12). Broad analysis of the long-term global anthropogenic seismic wavefield has been lacking. The impact of large, coherent changes in human behavior on seismic noise is unknown, as is how far it propagates and whether seismic recordings offer a coarse proxy for monitoring human activity patterns. Answering these questions has proven challenging: datasets are large, monitoring network heterogeneous, and the many possible noise sources likely vary spatially and overlap in time (13).

The COVID-19 outbreak was declared a global health emergency in January 2020 (14) and a pandemic in March by the World Health Organization. The outbreak resulted in emergency measures to reduce the basic reproduction rate of the virus (R_0) (15), beginning in China, Italy, and then followed by most countries. These measures disrupted social and economic behavior (16), industry (17), and tourism (18). In this paper, we use “lockdown” to broadly encompass many

types of emergency measures, such as full quarantine (e.g., Wuhan, China (19–21)), enforced physical distancing (e.g., Italy; UK), travel restrictions (22), widespread closure of services and industry, or any other emergency measures. These drastic changes to daily life provide a unique opportunity to study their environmental impacts, such as reductions in nitrous oxide emissions in the atmosphere (23). Recordings of human-generated seismic vibrations that travel through the solid Earth provide insights into the dynamics of pandemic lockdowns.

We assessed the effects of COVID-19 lockdowns on high-Frequency (4–14 Hz) Seismic Ambient Noise (hiFSAN; (24)). We compiled a global seismic noise dataset using vertical-component seismic waveform data from 337 broadband and individually operated citizen seismometer stations (24), such as Raspberry Shakes (RS), with a self-noise well below the ground motion generated by anthropogenic noise (25), and flat responses in the target frequency band (Fig. 1). For 268 seismic stations, we obtained usable data (e.g., no large data gaps, working sensors) and found significant reductions in hiFSAN during local lockdown measures at 185 stations (Fig. 2). Periods that are often seismically quiet include weekends, and the Christmas / New Year holidays for those locations where these are celebrated. We found a near-global reduction in noise, commencing in China in late Jan 2020, then followed by Europe and the rest of the world in Mar to Apr 2020. The noise level we observe during lockdowns lasted longer and was often quieter than the Christmas to New Year period.

In China (Fig. 3A), the COVID-19 outbreak and subsequent emergency measures occurred during Chinese New Year (CNY). In Enshi city, Hubei province, where the outbreak began (26), hiFSAN in 2020 clearly diverges from the normal annual reduction during CNY. The hiFSAN level remained at a minimum for several weeks after CNY. This minimum was demarcated by the start and end of quarantine in Hubei. While such strict quarantine measures were not enforced in Beijing, local hiFSAN reductions are stronger and longer than recent years. As of the end date of our analysis, Beijing has still not reached the average hiFSAN level of

previous years, suggesting the impact of COVID-19 is still restricting anthropogenic noise there. We noticed a later hiFSAN lockdown reduction in Apr 2020 in Heilongjiang, in NE China, near the Russian border.

While we see seismic effects of lockdown in areas with low population density estimates (<1 person per km^2 , Fig. 1), the strongest hiFSAN reduction occurs in populated environments. For a permanent seismic station in Sri Lanka, a 50% reduction in hiFSAN occurred after lockdown, the strongest we observed in the available data from that station since at least July 2013 (fig. S2). In Central Park, New York, on Sunday nights, hiFSAN was 10% lower during the lockdown compared to before it (fig. S3).

Seismic networks in populated areas allow us to correlate hiFSAN with other human activity measurements, such as audible recordings and flight data (24). At a surface station in Brussels, Belgium (Fig. 3B), we found a 33% reduction in hiFSAN after lockdown. We compared this with data from a nearby microphone, located close to a major road, that mainly records audible traffic noise. We found a high correlation between pre-lockdown hiFSAN and audible noise, both showing characteristic diurnal and weekly changes. However, during lockdown, audible noise reductions are more pronounced, suggesting that seismometers are sensitive to a wider distribution of seismic sources, not solely to the nearby traffic. Audible and hiFSAN levels then gradually increase after Apr 2020. Independent mobility data (24) provide insights into what cause these changes. Mobility correlates with hiFSAN at lockdown, with correlation coefficients exceeding 0.8 (24), except for time spent at places of residence (Google's "residential" category), which is expected given the increased number of people spending more time at home due to government restrictions.

Citizen seismometers provide a different urban ground motion dataset, with denser coverage in some places. Large hiFSAN drops especially occurred at schools and universities following lockdown-related closures (e.g., in Boston and Michigan (US) and Cornwall (UK)), fig. S4). The hiFSAN level is even 20% lower than during school holidays, indicating sensitivity to the environment outside of the school.

The pandemic impacted tourism, for example, during the holiday season in the Caribbean. In Barbados (Fig. 3C), hiFSAN decreased by $\sim 45\%$ following lockdown on 28 March 2020, through April 2020 and stayed $\sim 50\%$ below levels observed in previous years for the same period. However, seismic noise levels started to decrease 1–2 weeks before a local curfew started. Local flight data (24) imply travel to Barbados started decreasing after 21 March 2020 and the overall reduction in hiFSAN might be due in part to tourists repatriating. We also observed noise reductions due to reduced tourist activity at ski resorts in Europe (Zugspitze) and the US (Mammoth Mountain) (fig. S5).

While we saw lockdown effects most strongly at surface stations, we also detected them underground. Seismometers installed in boreholes to minimize the effects of anthropogenic noise on the data monitor potential hazards associated with the Auckland Volcanic Field, New Zealand (6, 8, 27). Station HBAZ is 380 m below the city, while MBAZ is at 98 m depth, 14 km from the city center on the uninhabited Motutapu island (Fig. 3D). The hiFSAN level at both stations varies between weekdays and weekends before the lockdown, suggesting that both are sensitive to anthropogenic activity. While the island station is quieter overall, the lockdown instigated a reduction in hiFSAN by a factor of 2 for both stations. We attribute the remaining hiFSAN maxima on the island (mid Apr 2020; early May 2020) to strong winds and high waves. On 27 April 2020, New Zealand lifted restrictions, with hiFSAN increasing to the pre-lockdown levels.

The reduction of hiFSAN is weaker in less populated areas, such as at Rundu which is located along the Namibia-Angola border (Fig. 3E). After COVID-19 was confirmed in Namibia, an emergency was declared on 17 Mar 2020 to restrict mobility, followed by full lockdown on 27 Mar 2020. These measures are reflected in $>25\%$ hiFSAN reduction compared to pre-lockdown. Despite Rundu having a population roughly 8 and 5 times less dense than Brussels and Auckland, respectively (28), we observed a similarly high correlation between seismic and mobility data. The Black Forest Observatory in Germany is an even more remote station, located 150–170 m below the surface in crystalline bedrock. Considered a reference low-noise laboratory (29), even there we found a small hiFSAN reduction during lockdown nights (fig. S6), corresponding to the lowest hiFSAN since at least 25 Dec 2015.

We have provided a global-scale analysis of high-frequency anthropogenic seismic noise. Global median hiFSAN dropped by as much as 50% during March to May 2020 (Fig. 4). The length and quiescence of this period represents the longest and most coherent global seismic noise reduction in recorded history, highlighting how human activities impact the solid Earth. A globally high correlation exists between changes in hiFSAN and population mobility (24), with correlations exceeding 0.9 for many categories.

This distinct low-noise period will help to optimize seismic monitoring (4). Analyzing the full spectrum of seismogenic behavior, including the smallest earthquakes, is essential for monitoring fault dynamics over seismic cycles, and for earthquake forecasting and seismic hazard assessment. Small earthquakes should dominate datasets (30), but typical operational catalogs using amplitude-based detection lack many of the smallest earthquakes (31). This detection issue is especially problematic in populated areas, where anthropogenic noise energy interferes with earthquake signals. This problem is exemplified by recordings of a M5.0 earthquake at 15 km depth SW of Petatlan, Mexico during

lockdown (fig. S7). An earthquake with this magnitude and source mechanism occurring during the daytime could typically only be observed at stations in urban environments by filtering the signal. However, the reduction of seismic noise by ~40% during lockdown made this event visible without any filtering required at a RS station in Querétaro city, 380 km away. Low noise levels during COVID-19 lockdowns could thus allow detection of signals from new sources in areas with incomplete seismic catalogs. Such newly identified signals could be used as distinct templates (30) for finding similar waveforms in noisier data pre- and post-lockdown. This approach also works for tremor signals masked by anthropogenic noise, yet vital for monitoring potential volcanic unrest (6). Although broadband sensors in rural environments are impacted less by anthropogenic noise, any densification of and reliance on low-cost sensors in urban areas, such as RS and low-cost accelerometers (32), will require a better understanding of anthropogenic noise sources to suppress false detections. As populations increase globally, more people become exposed to potential natural and induced geohazards (33). Urbanization will increase anthropogenic noise in exposed areas, further complicating seismic monitoring. Characterizing and minimizing anthropogenic noise is increasingly important for accurately detecting and imaging the seismic signatures of potentially harmful subsurface hazards.

Anthropogenic seismic noise is thought to be dominated by noise sources less than 1 km away (5–7, 11, 34). Because population mobility generates time-varying loads that radiate energy through the shallow subsurface as Rayleigh waves (11), local effects, such as construction sites, and heavy machinery, can impact individual stations. However, the unique 2020 seismic noise quiet period reveals that when considering multiple stations or whole networks over longer time-scales, the anthropogenic seismic wavefield affects large areas. With denser networks and more citizen sensors in urban environments, more features of the seismic noise, rather than just amplitude, will become usable and will help to identify different anthropogenic noise sources (10, 35). Characterizing these sources will be useful for imaging the shallow subsurface in 3D in urban areas using high-frequency anthropogenic ambient noise (36, 37). Our finding of a distributed noise field is supported by the strong correlations with independent mobility data (Fig. 4). In contrast to mobility data, publicly available data from existing seismometer networks provide an objective absolute baseline of human activity levels. Therefore, hiFSAN can serve as a near-real-time technique for monitoring anthropogenic activity patterns with fewer potential privacy concerns than mobility data. In addition, industrial activities may not be captured in mobility data, but leave a seismic noise signature. The 2020 seismic quiet period is a baseline for using seismic properties (34) to

identify and isolate the sources contributing to the anthropogenic noise wavefield, especially when combined with data indicative of human behavior. The seismic observations of human activity during the COVID-19 lockdown allow us to assess the impact of mitigation policies on daily life, especially the time to establish and recover from lockdowns. As such, hiFSAN may provide important constraints for health and behavioral science studies.

REFERENCES AND NOTES

1. J. N. Brune, J. Oliver, The seismic noise of the earth's surface. *Bull. Seismol. Soc. Am.* **49**, 349–353 (1959).
2. R. K. Cessaro, Sources of primary and secondary microseisms. *Bull. Seismol. Soc. Am.* **84**, 142–148 (1994).
3. N. M. Shapiro, M. Campillo, Emergence of broadband Rayleigh waves from correlations of the ambient seismic noise. *Geophys. Res. Lett.* **31**, L07614 (2004). [doi:10.1029/2004GL019491](https://doi.org/10.1029/2004GL019491)
4. D. E. McNamara, R. P. Buland, Ambient Noise Levels in the Continental United States. *Bull. Seismol. Soc. Am.* **94**, 1517–1527 (2004). [doi:10.1785/0120030001](https://doi.org/10.1785/0120030001)
5. J. C. Groos, J. R. Ritter, Time domain classification and quantification of seismic noise in an urban environment. *Geophys. J. Int.* **179**, 1213–1231 (2009). [doi:10.1111/j.1365-246X.2009.04343.x](https://doi.org/10.1111/j.1365-246X.2009.04343.x)
6. C. M. Boese, L. Wotherspoon, M. Alvarez, P. Malin, Analysis of Anthropogenic and Natural Noise from Multilevel Borehole Seismometers in an Urban Environment, Auckland, New Zealand. *Bull. Seismol. Soc. Am.* **105**, 285–299 (2015). [doi:10.1785/0120130288](https://doi.org/10.1785/0120130288)
7. D. N. Green, I. D. Bastow, B. Dashwood, S. E. Nippres, Characterizing Broadband Seismic Noise in Central London. *Seismol. Res. Lett.* **88**, 113–124 (2017). [doi:10.1785/0220160128](https://doi.org/10.1785/0220160128)
8. C. L. Ashenden, J. M. Lindsay, S. Sherburn, I. E. M. Smith, C. A. Miller, P. E. Malin, Some challenges of monitoring a potentially active volcanic field in a large urban area: Auckland volcanic field, New Zealand. *Nat. Hazards* **59**, 507–528 (2011). [doi:10.1007/s11069-011-9773-0](https://doi.org/10.1007/s11069-011-9773-0)
9. N. Riahi, P. Gerstoft, The seismic traffic footprint: Tracking trains, aircraft, and cars seismically. *Geophys. Res. Lett.* **42**, 2674–2681 (2015). [doi:10.1002/2015GL063558](https://doi.org/10.1002/2015GL063558)
10. N. J. Lindsey *et al.*, [arXiv:2005.04861](https://arxiv.org/abs/2005.04861) (2020).
11. J. Díaz, M. Ruiz, P. S. Sánchez-Pastor, P. Romero, Urban seismology: On the origin of earth vibrations within a city. *Sci. Rep.* **7**, 15296 (2017). [doi:10.1038/s41598-017-15499-y](https://doi.org/10.1038/s41598-017-15499-y) [Medline](https://www.ncbi.nlm.nih.gov/pubmed/29111111)
12. P. Denton, S. Fishwick, V. Lane, D. Daly, Football Quakes as a Tool for Student Engagement. *Seismol. Res. Lett.* **89**, 1902–1907 (2018). [doi:10.1785/0220180078](https://doi.org/10.1785/0220180078)
13. D. Wilson *et al.*, Broadband Seismic Background Noise at Temporary Seismic Stations Observed on a Regional Scale in the Southwestern United States. *Bull. Seismol. Soc. Am.* **92**, 3335–3342 (2002). [doi:10.1785/0120010234](https://doi.org/10.1785/0120010234)
14. C. Sohrabi *et al.*, World Health Organization declares global emergency: A review of the 2019 novel coronavirus (COVID-19). *Int. J. Surg.* **76**, 71–76 (2020). [doi:10.1016/j.ijsu.2020.02.034](https://doi.org/10.1016/j.ijsu.2020.02.034)
15. R. M. Anderson, H. Heesterbeek, D. Klinkenberg, T. D. Hollingsworth, How will country-based mitigation measures influence the course of the COVID-19 epidemic? *Lancet* **395**, 931–934 (2020). [doi:10.1016/S0140-6736\(20\)30567-5](https://doi.org/10.1016/S0140-6736(20)30567-5) [Medline](https://www.ncbi.nlm.nih.gov/pubmed/32179634)
16. M. Nicola *et al.*, Evidence based management guideline for the COVID-19 pandemic. *Int. J. Surg.* **77**, 206–216 (2020). [doi:10.1016/j.ijsu.2020.04.001](https://doi.org/10.1016/j.ijsu.2020.04.001)
17. T. Laing, The economic impact of the Coronavirus 2019 (Covid-2019): Implications for the mining industry. *Extr. Ind. Soc.* **7**, 580–582 (2020). [doi:10.1016/j.exis.2020.04.003](https://doi.org/10.1016/j.exis.2020.04.003)
18. A. Hoque, F. A. Shikha, M. W. Hasanat, I. Arif, A. B. A. Hamid, The Effect of Coronavirus (COVID-19) in the Tourism Industry in China. *Asian J. Multidiscip. Stud.* **3**, 52–58 (2020).
19. M. U. G. Kraemer, C.-H. Yang, B. Gutierrez, C.-H. Wu, B. Klein, D. M. Pigott, L. du Plessis, N. R. Faria, R. Li, W. P. Hanage, J. S. Brownstein, M. Layan, A. Vespignani, H. Tian, C. Dye, O. G. Pybus, S. V. Scarpino; Open COVID-19 Data Working Group,

- The effect of human mobility and control measures on the COVID-19 epidemic in China. *Science* **368**, 493–497 (2020). [doi:10.1126/science.abb4218](https://doi.org/10.1126/science.abb4218) [Medline](#)
20. H. Tian, Y. Liu, Y. Li, C.-H. Wu, B. Chen, M. U. G. Kraemer, B. Li, J. Cai, B. Xu, Q. Yang, B. Wang, P. Yang, Y. Cui, Y. Song, P. Zheng, Q. Wang, O. N. Bjornstad, R. Yang, B. T. Grenfell, O. G. Pybus, C. Dye, An investigation of transmission control measures during the first 50 days of the COVID-19 epidemic in China. *Science* **368**, 638–642 (2020). [doi:10.1126/science.abb6105](https://doi.org/10.1126/science.abb6105) [Medline](#)
 21. J. Zhang, M. Litvinova, Y. Liang, Y. Wang, W. Wang, S. Zhao, Q. Wu, S. Merler, C. Viboud, A. Vespignani, M. Ajelli, H. Yu, Changes in contact patterns shape the dynamics of the COVID-19 outbreak in China. *Science* **368**, 1481–1486 (2020). [doi:10.1126/science.abb8001](https://doi.org/10.1126/science.abb8001) [Medline](#)
 22. M. Chinazzi, J. T. Davis, M. Ajelli, C. Gioannini, M. Litvinova, S. Merler, A. Pastore Y Piontti, K. Mu, L. Rossi, K. Sun, C. Viboud, X. Xiong, H. Yu, M. E. Halloran, I. M. Longini Jr., A. Vespignani, The effect of travel restrictions on the spread of the 2019 novel coronavirus (COVID-19) outbreak. *Science* **368**, 395–400 (2020). [Medline](#)
 23. M. Bauwens, S. Compennolle, T. Stavrou, J.-F. Müller, J. Gent, H. Eskes, P. F. Levelt, R. A. J. P. Veefkind, J. Vlietinck, H. Yu, C. Zehner, Impact of Coronavirus Outbreak on NO₂ Pollution Assessed Using TROPOMI and OMI Observations. *Geophys. Res. Lett.* **47**, 11 (2020). [doi:10.1029/2020GL087978](https://doi.org/10.1029/2020GL087978)
 24. Materials and Methods, and Network Citations are available as supplementary materials.
 25. R. E. Anthony, A. T. Ringler, D. C. Wilson, E. Wolin, Do Low-Cost Seismographs Perform Well Enough for Your Network? An Overview of Laboratory Tests and Field Observations of the OSOP Raspberry Shake 4D. *Seismol. Res. Lett.* **90**, 219–228 (2019). [doi:10.1785/0220180251](https://doi.org/10.1785/0220180251)
 26. H. Lau *et al.*, The positive impact of lockdown in Wuhan on containing the COVID-19 outbreak in China. *J. Travel Med.* **27**, taaa037 (2020). [doi:10.1093/jtm/taaa037](https://doi.org/10.1093/jtm/taaa037)
 27. S. Sherburn, B. J. Scott, J. Olsen, C. Miller, Monitoring seismic precursors to an eruption from the Auckland Volcanic Field, New Zealand. *N. Z. J. Geol. Geophys.* **50**, 1–11 (2007). [doi:10.1080/00288300709509814](https://doi.org/10.1080/00288300709509814)
 28. Center for International Earth Science Information Network CIESIN Columbia University, Gridded population of the world, version 4 (GPWv4): Population density. Revision 11, Accessed 2 June 2020 (2018); <https://doi.org/10.7927/H49C6VHW>
 29. W. Zürn, J. ExB, H. Steffen, C. Kroner, T. Jahr, M. Westerhaus, On reduction of long-period horizontal seismic noise using local barometric pressure. *Geophys. J. Int.* **171**, 780–796 (2007). [doi:10.1111/j.1365-246X.2007.03553.x](https://doi.org/10.1111/j.1365-246X.2007.03553.x)
 30. B. Gutenberg, C. F. Richter, Frequency of earthquakes in California. *Bull. Seismol. Soc. Am.* **34**, 185–188 (1944).
 31. Z. E. Ross, D. T. Trugman, E. Hauksson, P. M. Shearer, Searching for hidden earthquakes in Southern California. *Science* **364**, 767–771 (2019). [doi:10.1126/science.aaw6888](https://doi.org/10.1126/science.aaw6888) [Medline](#)
 32. E. S. Cochran, To catch a quake. *Nat. Commun.* **9**, 2508 (2018). [doi:10.1038/s41467-018-04790-9](https://doi.org/10.1038/s41467-018-04790-9) [Medline](#)
 33. G. J. H. McCall, Geohazards and the urban environment. *Geol. Soc. London Eng. Geol. Spec. Publ.* **15**, 309–318 (1998). [doi:10.1144/GSL.ENG.1998.015.01.31](https://doi.org/10.1144/GSL.ENG.1998.015.01.31)
 34. M. Lehujeur, J. Vergne, J. Schmittbuhl, A. Maggi, Characterization of ambient seismic noise near a deep geothermal reservoir and implications for interferometric methods: A case study in northern Alsace, France. *Geotherm. Energy* **3**, 3 (2015). [doi:10.1186/s40517-014-0020-2](https://doi.org/10.1186/s40517-014-0020-2)
 35. G. Hillers, M. Campillo, Y.-Y. Lin, K.-F. Ma, P. Roux, Anatomy of the high-frequency ambient seismic wave field at the TCDP borehole. *J. Geophys. Res.* **117**, B06301 (2012). [doi:10.1029/2011JB008999](https://doi.org/10.1029/2011JB008999)
 36. M. Picozzi, S. Parolai, D. Bindi, A. Strollo, Characterization of shallow geology by high-frequency seismic noise tomography. *Geophys. J. Int.* **176**, 164–174 (2009). [doi:10.1111/j.1365-246X.2008.03966.x](https://doi.org/10.1111/j.1365-246X.2008.03966.x)
 37. F. Brenguier, P. Boué, Y. Ben-Zion, F. Vernon, C. W. Johnson, A. Mordret, O. Coutant, P.-E. Share, E. Beaucé, D. Hollis, T. Lecocq, Train Traffic as a Powerful Noise Source for Monitoring Active Faults With Seismic Interferometry. *Geophys. Res. Lett.* **46**, 9529–9536 (2019). [doi:10.1029/2019GL083438](https://doi.org/10.1029/2019GL083438) [Medline](#)
 38. T. Lecocq *et al.*, ThomasLecocq/2020_Science_GlobalQuieting: First Release - v1.0, Zenodo (2020) <https://doi.org/10.5281/zenodo.3944739>
 39. A. Aktay *et al.*, [arXiv:2004.04145](https://arxiv.org/abs/2004.04145) (2020).
 40. M. Schäfer, M. Strohmeier, V. Lenders, I. Martinovic, M. Wilhelm, IPSN-14 Proceedings of the 13th International Symposium on Information Processing in Sensor Networks (IEEE, 2014), pp. 83–94.
 41. S. R. Proud, Go-Around Detection Using Crowd-Sourced ADS-B Position Data. *Aerospace* **7**, 16 (2020). [doi:10.3390/aerospace7020016](https://doi.org/10.3390/aerospace7020016)
 42. D. E. McNamara, R. I. Boaz, U.S. Geol. Surv. Open-File Rept 2010-1292, 41 (2010).
 43. R. E. Anthony, A. T. Ringler, D. C. Wilson, M. Bahavar, K. D. Koper, How Processing Methodologies Can Distort and Bias Power Spectral Density Estimates of Seismic Background Noise. *Seismol. Res. Lett.* **91**, 1694–1706 (2020). [doi:10.1785/0220190212](https://doi.org/10.1785/0220190212)
 44. M. Beyreuther, R. Barsch, L. Krischer, T. Megies, Y. Behr, J. Wassermann, ObsPy: A Python Toolbox for Seismology. *Seismol. Res. Lett.* **81**, 530–533 (2010). [doi:10.1785/gssrl.81.3.530](https://doi.org/10.1785/gssrl.81.3.530)
 45. T. Megies, M. Beyreuther, R. Barsch, L. Krischer, J. Wassermann, ObsPy – What can it do for data centers and observatories? *Ann. Geophys.* **54**, 47–58 (2011). [doi:10.4401/ag-4838](https://doi.org/10.4401/ag-4838)
 46. L. Krischer, T. Megies, R. Barsch, M. Beyreuther, T. Lecocq, C. Caudron, J. Wassermann, ObsPy: A bridge for seismology into the scientific Python ecosystem. *Comput. Sci. Discov.* **8**, 014003 (2015). [doi:10.1088/1749-4699/8/1/014003](https://doi.org/10.1088/1749-4699/8/1/014003)
 47. R. B. Blackman, J. W. Tukey, The measurement of power spectra from the point of view of communications engineering—Part I. *Bell Syst. Tech. J.* **37**, 185–282 (1958). [doi:10.1002/j.1538-7305.1958.tb03874.x](https://doi.org/10.1002/j.1538-7305.1958.tb03874.x)
 48. P. Welch, The use of fast Fourier transform for the estimation of power spectra: A method based on time averaging over short, modified periodograms. *IEEE Trans. Audio Electroacoust.* **15**, 70–73 (1967). [doi:10.1109/TAU.1967.1161901](https://doi.org/10.1109/TAU.1967.1161901)
 49. J. D. Hunter, Matplotlib: A 2D Graphics Environment. *Comput. Sci. Eng.* **9**, 90–95 (2007). [doi:10.1109/MCSE.2007.55](https://doi.org/10.1109/MCSE.2007.55)
 50. R. Lacassin, M. Devès, S. P. Hicks, J.-P. Ampuero, R. Bossu, L. Bruhat, D. F. Wibisono, L. Fallou, E. J. Fielding, A.-A. Gabriel, J. Gurney, J. Krippner, A. Lomax, M. M. Sudibyo, A. Pamumpuni, J. R. Patton, H. Robinson, M. Tingay, S. Valkanotis, Rapid collaborative knowledge building via Twitter after significant geohazard events. *Geosci. Commun.* **3**, 129–146 (2020). [doi:10.5194/gc-3-129-2020](https://doi.org/10.5194/gc-3-129-2020)
 51. T. Kluyver *et al.*, Positioning and Power in Academic Publishing: Players, Agents and Agendas, F. Loizides, B. Schmidt, eds. (IOS Press, 2016), pp. 87–90.
 52. T. Lecocq, F. Massin, C. Satriano, M. Vanstone, T. Megies, SeismoRMS - A simple Python/Jupyter Notebook package for studying seismic noise changes (2020).
 53. L. Krischer, Y. A. Aiman, T. Bartholomaeus, S. Donner, M. Driel, K. Duru, K. Garina, K. Gessle, T. Gunawan, S. Hable, C. Hadzioannou, M. Koymans, J. Leeman, F. Lindner, A. Ling, T. Megies, C. Nunn, A. Rijal, J. Salvermoser, S. T. Soza, C. Tape, T. Taufiqurrahman, D. Vargas, J. Wassermann, F. Wöfl, M. Williams, S. Wollherr, H. Igel, seismo-live: An Educational Online Library of Jupyter Notebooks for Seismology. *Seismol. Res. Lett.* **89**, 2413–2419 (2018). [doi:10.1785/0220180167](https://doi.org/10.1785/0220180167)
 54. QGIS Development Team, QGIS Geographic Information System, Open Source Geospatial Foundation (2020).

ACKNOWLEDGMENTS

We sincerely thank the editor, two anonymous reviewers, Tarje Nissen-Meyer, and Janet Slate for their comments, which have improved the manuscript. We are extremely grateful to all seismic network managers, operators, and technicians who have helped to facilitate the raw global seismic dataset (24). We also kindly acknowledge all the passionate community seismologists for running their “home” seismometers and participating, indirectly, to a better understanding of the Earth. Any use of trade, firm, or product names is for descriptive purposes only and does not imply endorsement by the U.S. Government. We dedicate this community-led study to all essential workers who have kept our countries going during these difficult times. **Funding:** P.K. was funded by a Royal Society University Research Fellowship (URF\R1\180377). P.B. and M.J. acknowledge support from the International Training Course “Seismology and Seismic Hazard Assessment” funded by the GeoForschungsZentrum Potsdam (GFZ) and the German Federal Foreign Office through the German Humanitarian Assistance program (grant S08-60 321.50 ALL 03/19). P.B. also acknowledges financial support from the Boğaziçi University Research Fund (BAP 15683). O.F.C.d.O. acknowledges funding from a Young Investigator Grant from the Human Frontier Science Program (HFSP - project number RGY0072/2017). C.P.E. and E.S.

acknowledge funding from the HELPOS Project “Hellenic Plate Observing System” (MIS 5002697). L.E. and S.S.-K. acknowledge funding from a VIDI project from the Dutch Research Council (NWO project number 864.14.005). G.A.F. acknowledges contributions from the Observatorio San Calixto, which is supported by the Air Force Technical Application Center (AFTAC). C.R.L. acknowledge funding from the NSF Graduate Research Fellowship Program (grant No. DGE-1745301). V.-H.M. and R.D.P. acknowledge support from grant CONACYT-299766. R.D.P. acknowledges support from the UNAM-DGAPA postdoctoral scholarship. J.O. acknowledges support from the Agencia Nacional de Investigación y Desarrollo (Scholarship ANID-PFCHA / Doctorado Nacional / 2020-21200903). S.P. acknowledges financial support from the Natural Environment Research Council (NE/R013144/1). A.E.R. acknowledges support from the K.H. Renlund foundation. M.K.S. acknowledges the New Zealand Earthquake Commission (EQC Project No 20796). H.X. acknowledges support from a Multidisciplinary Research on the Coronavirus and its Impacts (MRCI) grant from UC Santa Barbara. The Australian Seismometers in Schools data used in this research are supported by AuScope, enabled by the Australian Commonwealth NCRIS program. A.O. acknowledges support from the project RESIST, funded by the Belgian Federal Science Policy (contract SR/00/305) and the Luxembourg National Research Fund. **Author contributions:** TL designed and led the research; TL, SH, KVN, KvW, PK and RDP processed and visualized the data and drafted the manuscript; FM contributed to the software development and provided the Supplementary video; GH thoroughly edited and reviewed the manuscript. All 76 authors processed seismic data, took part in discussions, and performed a full interactive review of the original and revised manuscripts. **Competing interests:** The authors declare no competing interests. **Data and materials availability:** The raw data used to compute the hiFSAN were obtained from different networks and data providers (24). The computed data and codes used to analyze and plot Figs. 1 to 4 are available from the companion repository (38): https://github.com/ThomasLecocq/2020_Science_GlobalQuieting (last accessed July 2020)

SUPPLEMENTARY MATERIALS

science.sciencemag.org/cgi/content/full/science.abd2438/DC1

Materials and Methods

Supplementary Text

Figs. S1 to S9

Tables S1 to S3

References (39–54)

Movie S1

10 June 2020; accepted 14 July 2020

Published online 23 July 2020

10.1126/science.abd2438

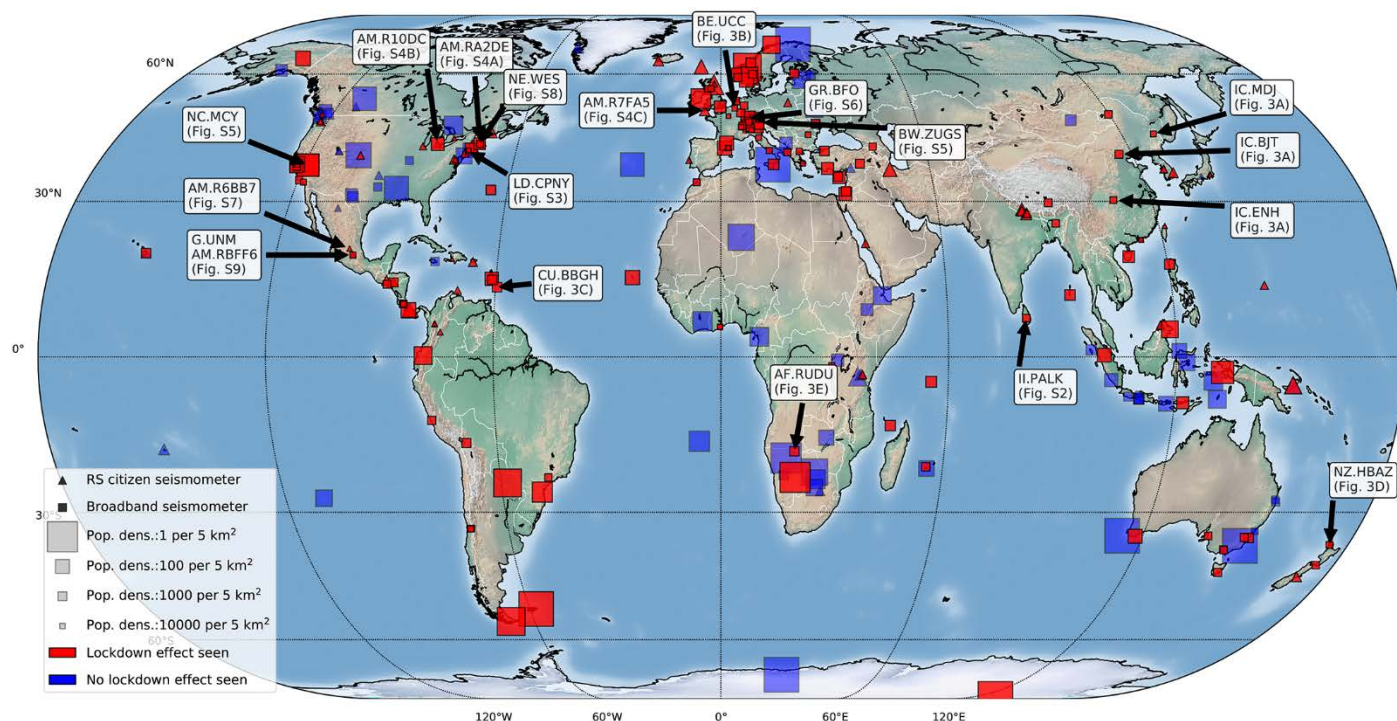


Fig. 1. Worldwide seismic station locations. Locations of the 268 global seismic stations with usable data (e.g., no long data gaps, working sensors) we analyzed. Lockdown effects are observed (red) at 185 out of 268 stations. Symbol size is scaled by the inverse of population density (28) to emphasize stations located in remote areas. The stations we labeled are discussed in detail in the text.

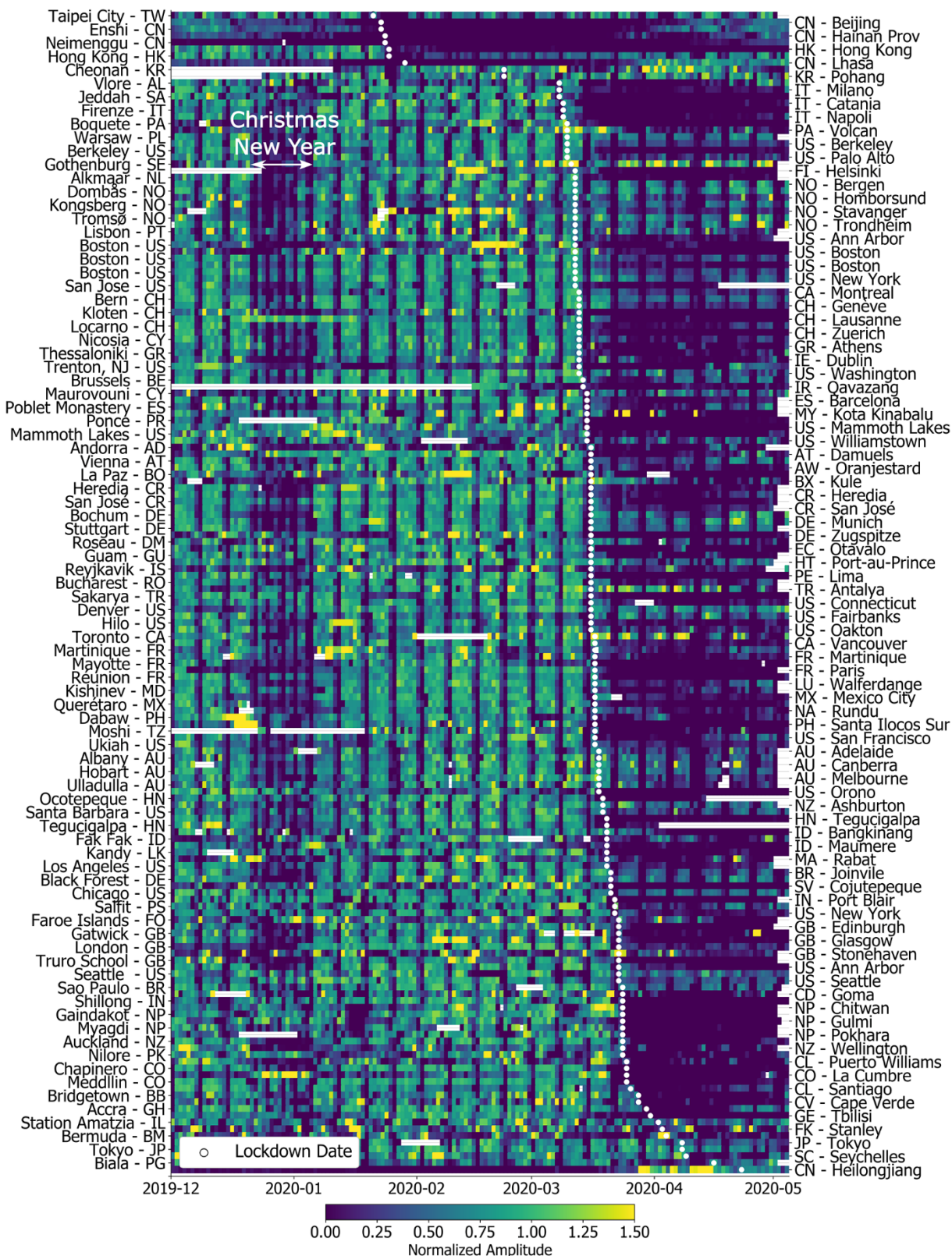


Fig. 2. Global temporal changes in seismic noise. Global daily median hiFSAN based on displacement data (24), normalized to percentage variation of the baseline before lockdown measures, and sorted by lockdown date. Data gaps are colored white. Location and country code of the station are indicated, while fig. S1 also includes the network and station code.

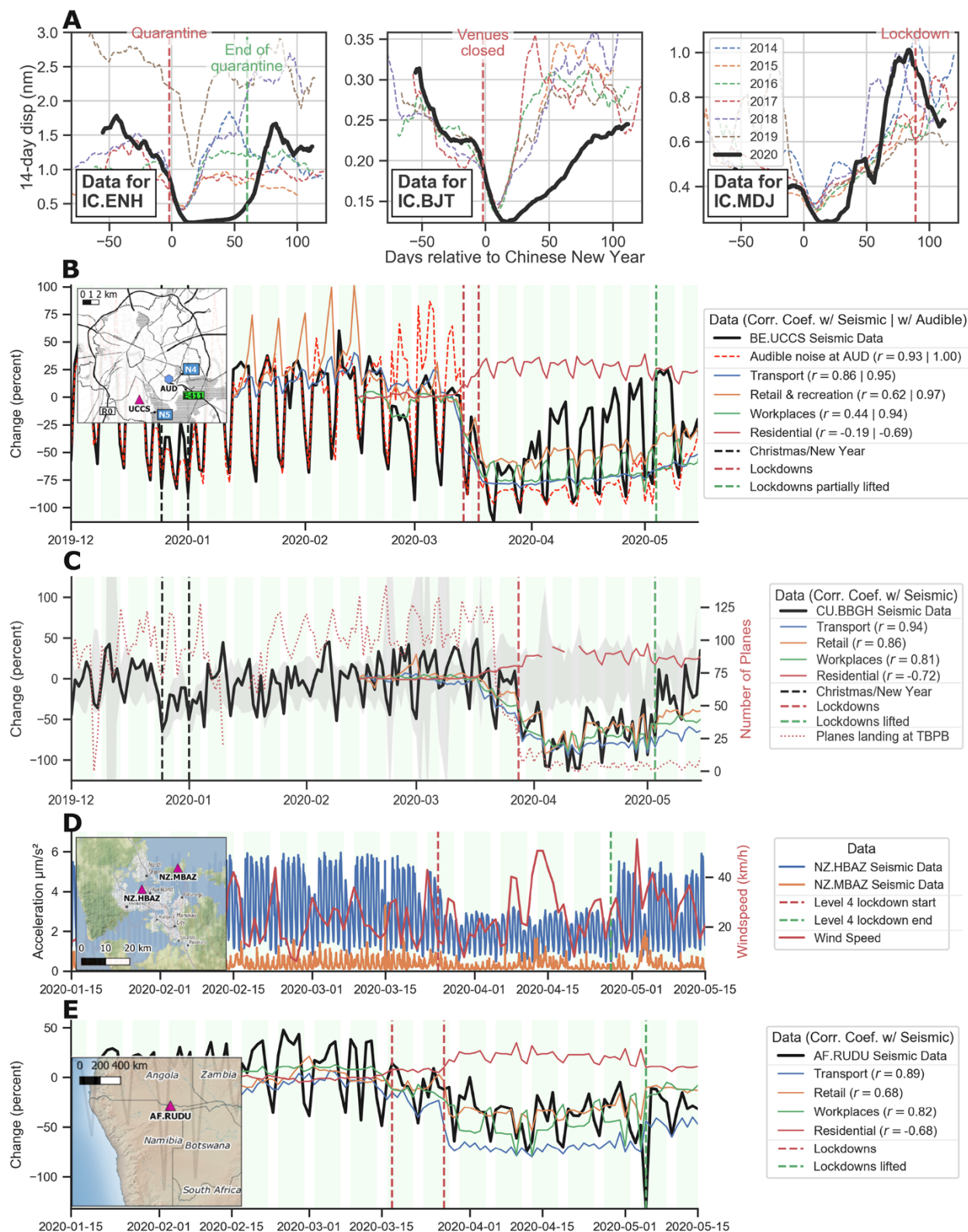


Fig. 3. Regional examples of the 2020 seismic noise quiet period. Examples showing different features of the lockdown seismic signal changes in regional settings. We filtered the hiFSAN data between 4 and 14 Hz and present temporal changes either as displacement (A), acceleration (D) or as percentage change compared to the baseline before lockdown (B, C and E) with the panels in (A) also comparing to the baseline of corresponding time periods in prior years. Individual seismic stations are identified by network.station codes (IC.ENH, BE.UCCS, etc.). The legends of (B-E) include correlation coefficients r with mobility data (24). (A) Lockdown effects at three stations in China compared to the Chinese New Year holiday in previous years. (B) Lockdown effects in hiFSAN compared with audible environmental noise and independent mobility data in Brussels, Belgium. (C) Lockdown effect in Barbados compared to noise levels in the last decade (in gray) and correlation with local flight data at the Grantley Adams International Airport (TBPB) (24). (D) Lockdown noise reduction recorded on borehole seismometers in Auckland, New Zealand. (E) Lockdown noise reduction in a region of low population density in Rundu, Namibia.

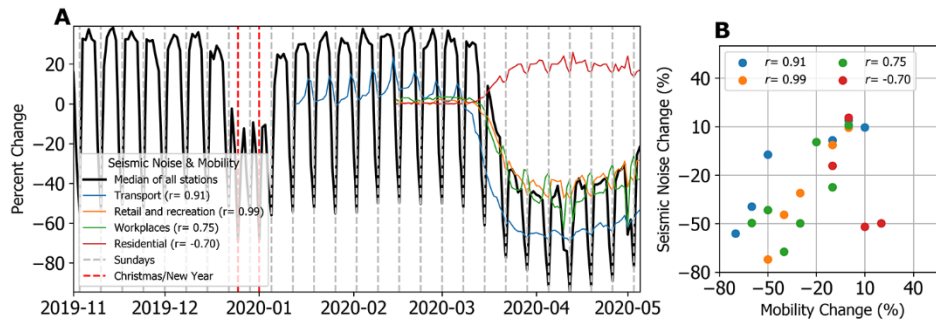


Fig. 4. Global changes in seismic noise compared to population mobility trends. (A) Comparison between temporal changes in global daily median hiFSAN based on the 185 stations that observed lockdown effects and population mobility changes (24). (B) Scatter-plot to illustrate the correlation between the binned (10% bins) time series of seismic noise changes and all categories of mobility data in (A). Percentage changes are given relative to a pre-lockdown baseline. All categories show a strong positive correlation, apart from time spent in residential premises, which is anti-correlated.

Global quieting of high-frequency seismic noise due to COVID-19 pandemic lockdown measures

Thomas Lecocq, Stephen P. Hicks, Koen Van Noten, Kasper van Wijk, Paula Koelemeijer, Raphael S. M. De Plaen, Frédéric Massin, Gregor Hillers, Robert E. Anthony, Maria-Theresia Apoloner, Mario Arroyo-Solórzano, Jelle D. Assink, Pinar Büyükkakpınar, Andrea Cannata, Flavio Cannavo, Sebastian Carrasco, Corentin Caudron, Esteban J. Chaves, David G. Cornwell, David Craig, Olivier F. C. den Ouden, Jordi Diaz, Stefanie Donner, Christos P. Evangelidis, Láslo Evers, Benoit Fauville, Gonzalo A. Fernandez, Dimitrios Giannopoulos, Steven J. Gibbons, Társilo Girona, Bogdan Grecu, Marc Grunberg, György Hetényi, Anna Horleston, Adolfo Inza, Jessica C. E. Irving, Mohammadreza Jamalreyhani, Alan Kafka, Mathijs R. Koymans, Celeste R. Labedz, Eric Larose, Nathaniel J. Lindsey, Mika McKinnon, Tobias Megies, Meghan S. Miller, William Minarik, Louis Moresi, Víctor H. Márquez-Ramírez, Martin Möllhoff, Ian M. Nesbitt, Shankho Niyogi, Javier Ojeda, Adrien Oth, Simon Proud, Jay Pulli, Lise Retailleau, Annukka E. Rintamäki, Claudio Satriano, Martha K. Savage, Shahr Shani-Kadmiel, Reinoud Sleeman, Efthimios Sokos, Klaus Stammler, Alexander E. Stott, Shiba Subedi, Mathilde B. Sørensen, Taka'aki Taira, Mar Tapia, Fatih Turhan, Ben van der Pluijm, Mark Vanstone, Jerome Vergne, Tommi A. T. Vuorinen, Tristram Warren, Joachim Wassermann and Han Xiao

published online July 23, 2020

ARTICLE TOOLS

<http://science.sciencemag.org/content/early/2020/07/22/science.abd2438>

SUPPLEMENTARY MATERIALS

<http://science.sciencemag.org/content/suppl/2020/07/22/science.abd2438.DC1>

RELATED CONTENT

<http://science.sciencemag.org/content/sci/369/6509/1299.full>

REFERENCES

This article cites 49 articles, 14 of which you can access for free
<http://science.sciencemag.org/content/early/2020/07/22/science.abd2438#BIBL>

PERMISSIONS

<http://www.sciencemag.org/help/reprints-and-permissions>

Use of this article is subject to the [Terms of Service](#)

Science (print ISSN 0036-8075; online ISSN 1095-9203) is published by the American Association for the Advancement of Science, 1200 New York Avenue NW, Washington, DC 20005. The title *Science* is a registered trademark of AAAS.

Copyright © 2020, American Association for the Advancement of Science